

AperTO - Archivio Istituzionale Open Access dell'Università di Torino

## Field measurements based model for surface irrigation efficiency assessment

### **This is the author's manuscript**

*Original Citation:*

*Availability:*

This version is available <http://hdl.handle.net/2318/1533668> since 2015-12-16T11:24:26Z

*Published version:*

DOI:10.1016/j.agwat.2015.03.015

*Terms of use:*

Open Access

Anyone can freely access the full text of works made available as "Open Access". Works made available under a Creative Commons license can be used according to the terms and conditions of said license. Use of all other works requires consent of the right holder (author or publisher) if not exempted from copyright protection by the applicable law.

(Article begins on next page)

# 1 FIELD MEASUREMENTS BASED MODEL FOR SURFACE 2 IRRIGATION EFFICIENCY ASSESSMENT

3 *D. Canone<sup>1\*</sup>, M. Previati<sup>1</sup>, I. Bevilacqua<sup>1</sup>, L. Salvai<sup>1</sup>, S. Ferraris<sup>1,2</sup>*

4 <sup>1</sup> Interuniversity Department of Regional and Urban Studies and Planning (DIST), Politecnico di Torino and Università  
5 di Torino, Castello del Valentino, viale Mattioli, 39, 10125 Torino, Italy

6 <sup>2</sup> ISAC-CNR, Istituto di Scienze dell'Atmosfera e del Clima, Corso Fiume 4, 10133 Torino, Italy

7 \*Corresponding author: [davide.canone@unito.it](mailto:davide.canone@unito.it), Ph: +390110907428, +393405995796

## 8 **Abstract**

9 Within scenarios of water scarcity, the irrigation efficiency plays an increasingly strategic role. In  
10 this paper, a method that uses an advance-infiltration model based on four field measurements and  
11 the soil particle size distribution is proposed to estimate border-irrigation efficiencies. This method  
12 was applied to fifteen irrigation events and the application, storage and distribution efficiencies  
13 were estimated. The advance-infiltration model was validated against soil moisture measurements.  
14 The field-scale saturated hydraulic conductivity was estimated by model fitting to the measured  
15 depth of water infiltration. The sensitivity of the modelled irrigation efficiency to the operational  
16 surface irrigation parameters was evaluated by simulating seven irrigation scenarios based on field-  
17 collected data.

18 The infiltration profiles obtained by the proposed method were in agreement with the soil moisture  
19 measurements. The maximum difference between simulated and measured infiltration depth was  
20 0.018 m . The field-scale saturated hydraulic conductivity values were in agreement with the  
21 infiltrometer tests results. The analysis of both simulated scenarios and monitored irrigation events  
22 highlighted the need for farmers to reduce the flow rates and increase the duration of irrigation  
23 events, in order to improve the irrigation efficiencies.

24 **Keywords:** agricultural hydrology; surface irrigation; irrigation efficiency; irrigation modelling.

## 25 **1 Introduction**

26 Because of the ever-increasing demand for water, analyses of irrigation efficiency have assumed an  
27 important role in Italy and throughout the entire Mediterranean area (Chohin-Kuper et al., 2003;  
28 Fereres and Soriano, 2007; Inglesias et al., 2007). Additionally, climate change is expected to  
29 increase water scarcity (Arnell, 1999; Inglesias et al., 2007).

30 On the western Po River Plain (Piedmont, northern Italy), where corn (*Zea mays* L.) is the most  
31 widely grown crop, surface irrigation systems are primarily used. Thus, for water resource  
32 management programmes (for which it is necessary to evaluate and reach a compromise between  
33 the constraints imposed by water scarcity and the production requirements) the analysis of the  
34 irrigation efficiencies of surface irrigation systems has become an essential tool.

35 To calculate the dependence of irrigation efficiency on irrigation parameters, three different  
36 strategies may be adopted: i) a detailed simulation of infiltration (e.g., Manzini and Ferraris, 2004;  
37 Ferraris et al., 2012); ii) a detailed simulation of infiltration coupled with the surface advance of  
38 water (e.g., Gandolfi and Savi, 2000); and iii) an analytical solution to the Lewis and Milne (1938)  
39 integral equation (Philip and Farrell, 1964).

40 Because the latter strategy requires a low number of parameters, it is suitable for providing a field-  
41 scale description of the rates of water advance and infiltration for practical uses (such as managing  
42 irrigation performance). In particular, when related to an infiltration function such as that of Philip  
43 (1957), which considers the saturated hydraulic conductivity, the Philip and Farrell analytical  
44 solution solves the advance-infiltration problem.

45 Although the Philip and Farrell analytical solution is only valid for short irrigation durations and  
46 cannot accurately predict long-term behaviour (Knight, 1980), this solution has been employed by  
47 several authors to successfully describe the advance-infiltration problem for surface irrigation  
48 management (e.g., Collis-George and Freebairn, 1979; Or and Silva, 1996).

49 The Philip (1957) infiltration function, used in the Philip and Farrell (1964) analytical solution,  
50 requires knowledge of soil hydraulic parameters to estimate the soil infiltration dynamics. Several  
51 authors have indicated that the Beerkan Estimation of Soil pedoTransfer (BEST) infiltration test

52 proposed by Lassabatère et al. (2006) is an effective method for the hydraulic characterisation of  
53 soils directly in the field (e.g., Mubarak et al., 2009; Xu et al., 2009; Bagarello et al., 2011).  
54 Bagarello et al. (2011) investigated the possibility of simplifying the particle size distribution curve  
55 (PSD) fitting by including only three points (the clay, silt and sand contents) instead of fourteen  
56 points. These authors found the simplified PSD to be a reliable alternative to the normal procedure.  
57 Other methods have been recently developed for irrigation and management purposes (e.g.: Bautista  
58 et al., 2009; Strelkoff et al., 2009), which use surface water depth and mass balance methods to  
59 estimate the infiltration. Also, an interesting new analytical solution has been developed (Cook et  
60 al., 2013). However, it is beyond the scope of this paper to compare different analytical solutions.  
61 The proposed method is based on the direct measurement of the infiltration depth to calibrate the  
62 infiltration advance model, and to estimate the saturated hydraulic conductivity at the field scale.  
63 Within the context of this the above mentioned simplification, this study aims to propose a method  
64 for the calculation of border-irrigation efficiencies by using an advance-infiltration model and four  
65 simple field measurements: i) the inflow rate; ii) the irrigation duration; iii) the water head imposed  
66 on the field surface during an irrigation event and iv) the monitoring of the soil water content at  
67 only one point in the field at only the beginning and the end of the irrigation process. The second  
68 objective of this study was to use the proposed method to evaluate the surface irrigation efficiency  
69 of irrigation events based on the actual practices adopted by farmers. Hence, this method can  
70 provide a simulation tool that is able to analyse the effects of differences in management practices  
71 on irrigation efficiency.

## 72 **2 Methodology**

### 73 *2.1 Advance-infiltration models*

74 Irrigation efficiencies depend on the volume of water infiltrated during the irrigation event and on  
75 the distribution of the infiltrated water across the field. To compute the infiltrated volume of water  
76 and assess its distribution, it is necessary to determine the infiltration profile across the field. This

77 infiltration profile can be obtained from the solution of the infiltration advance across the field. The  
 78 infiltration advance is calculated from the simultaneous solution of two equations: the analytical  
 79 solution to the Lewis-Milne (1938) differential equation proposed by Philip and Farrell (1964) to  
 80 describe the advance of the water front and the infiltration equation of Philip (1957). These two  
 81 equations are written as:

$$82 \quad \frac{x}{q} = \frac{1}{C} \left[ 1 - \exp\left(\frac{4C^2 t}{\pi \cdot S^2}\right) \operatorname{erfc} \frac{2Ct^{1/2}}{\pi^{1/2} S} \right], \text{ and} \quad (1)$$

$$83 \quad I = S\sqrt{t} + Ct, \quad (2)$$

84 where,  $x$  (L) is the horizontal spatial coordinate of the water advance front;  $q$  ( $L^2 T^{-1}$ ) is the inflow  
 85 rate per unit of width;  $C$  ( $L T^{-1}$ ) is a parameter related to the saturated hydraulic conductivity  $K_s$  ( $L$   
 86  $T^{-1}$ ) according to the relation proposed by Haverkamp et al. (1988):

$$87 \quad \frac{1}{3} K_s \leq C \leq \frac{2}{3} K_s, \quad (3)$$

88 which depends on the initial soil water content;  $t$  (T) is the time;  $S$  ( $L T^{-1/2}$ ) is the sorptivity;  $I$  (L) is  
 89 the cumulative infiltration at any chosen value of  $x$ .

90 In this study, the parameter  $C$  was considered as constant and equal to  $K_s/2$ , as suggested by  
 91 Parlange (1977). Such an assumption is valid because  $C$  is only slightly dependent on the initial  
 92 water content (Philip 1957), and for most practical purposes, any change in  $C$  may be neglected.  
 93 This assumption is not made because  $C$  does not change, but the changes in  $C$  are relevant for long-  
 94 term infiltration rates, which are not considered in this work, and may be caused by changes in the  
 95 saturated hydraulic conductivity (Samani and Yitayew 1989; Silva 1995) in association with  
 96 changes in the near-surface soil porosity. Because long-term infiltration rates are not considered in  
 97 this work, the Philip and Farrel analytical solution can be applied. In fact, the Philip and Farrell  
 98 analytical solution should only be considered valid for short irrigation durations and should not be  
 99 applied to accurately predict long-term behaviour (Knight, 1980). The method proposed by Knight

100 (1980) to verify short-duration conditions has been adopted in this work and is presented in the  
 101 following section.

102 Sorptivity is defined as a function of the scale parameters of the water retention and hydraulic  
 103 conductivity curves according to the relationship proposed by Parlange (1975):

$$104 \quad S^2 = \int_{\theta_i}^{\theta_s} (\theta_s + \theta - 2\theta_i) K \frac{dh}{d\theta} d\theta \quad (4)$$

105 where,  $\theta_s$  ( $L^3 L^{-3}$ ) is the soil water content at saturation;  $\theta$  ( $L^3 L^{-3}$ ) is the actual soil water content;  $\theta_i$   
 106 ( $L^3 L^{-3}$ ) is the initial soil water content;  $K$  ( $L T^{-1}$ ) is the soil hydraulic conductivity at  $\theta$ ;  $h$  (-L) is the  
 107 actual matric potential.

108 In this study, the van Genuchten (1980) equation and the Brooks and Corey (1964) relationship  
 109 were chosen as the models for calculating the water retention and hydraulic conductivity,  
 110 respectively. The effect of hysteresis on the water retention curve was neglected, but it can be  
 111 incorporated by including a hysteresis model, as suggested by Canone et al., 2008.

112 Hence, by integrating Eq. (4) within the water content range, one obtains:

$$113 \quad S^2 = (\theta_i, \theta_s) = -C_p \theta_s K_S h_g \left( 1 - \frac{\theta_i}{\theta_s} \right) \left[ 1 - \left( \frac{\theta_i}{\theta_s} \right)^\eta \right] \quad (5)$$

114 Where,  $h_g$  (-L) is the matric potential scale parameter of the van Genuchten (1980) equation;  $K_S$  ( $L$   
 115  $T^{-1}$ ) and  $\eta$  ( $L$ ) are the scale parameter and shape parameter of the Brooks and Corey (1964)  
 116 equation;  $C_p$  (-) is a soil-dependent constant (Haverkamp et al., 2006) depending on the shape  
 117 parameters  $m$  and  $n$  of the van Genuchten (1980) equation.

118 Equation (1) is a function of  $S$ ,  $K_S$  and  $q$ , and equation (2) is function of  $S$  and  $K_S$ . Since the method  
 119 was applied to estimate the irrigation efficiency of border irrigation, the flow rate was measured at  
 120 the inlet of a bay located at the centre of the field. The flow rate ( $q$ ) was assessed by measurement  
 121 of the cross-sectional area and the measurement of the current velocity. The latter was determined  
 122 with a propeller flow meter OTT C2 (OTT Hydromet, Kempten, Germany, UE), which was

123 installed before any irrigation monitoring and removed at the end of it.  $S$  and  $K_S$  are not directly  
124 measurable. In the proposed approach, the sorptivity is computed by solving equation (5), which  
125 requires the values of  $\theta_s$ ,  $\theta_i$ ,  $K_S$ ,  $h_g$ ,  $\eta$ ,  $m$  and  $n$ .

126 The soil water content at saturation and the initial soil water content were measured at a time  
127 domain reflectometry (TDR) station located at one point in the field. The matric potential scale  
128 parameter ( $h_g$ ) was calculated using the soil-independent conceptual model proposed by  
129 Vanclouster et al. (2011) to predict the soil water retention curve from the cumulative particle size  
130 distribution (PSD) curve and the void ratio.

131 In this study, the shape parameters  $m$ ,  $n$  and  $\eta$  were determined from the PSD curve as suggested by  
132 Haverkamp et al., 2002. The PSD curve was fitted to five points obtained from the analysis of soil  
133 samples collected at an upstream, a centre and a downstream position along the bay under study.  
134 The particle size analysis was performed according to the pipette method, which is based on the  
135 difference in sedimentation speed between small and large soil particles. As demonstrated by  
136 Bagarello et al. (2011), the use of five points to fit a cumulative particle size distribution curve is  
137 sufficient for determining soil hydraulic parameters.

138 In the proposed approach, the saturated hydraulic conductivity ~~is~~ was the only parameter that cannot  
139 be measured. The field-equivalent value ( $K_{Seq}$ ) ~~is~~ was determined by model fitting. Equations (1)  
140 and (2) were fitted to the depth of water infiltration at the end of an irrigation event. In Eqs. (1) and  
141 (2)  $C$  was considered equal to  $0.5K_{Seq}$  and  $S$  was replaced by Eq. (5), so that only  $K_{Seq}$  was obtained  
142 by model fitting. The depth of water infiltration ~~is~~ was calculated from the water content data  
143 measured at the TDR station at the start and at the end of the irrigation event, following the  
144 methodology presented in section 2.5. The advance-infiltration model was validated against four  
145 depths of water infiltration at four times in-between the start and the end of the irrigation event.

146 The differences between the simulated ( $I_s$ ) and measured ( $I_m$ ) infiltration depth were compared to  
147 Cook et al. (2013) results employing the square root of the Nash-Sutcliffe efficiency coefficient  
148 (Nash and Sutcliffe, 1970), given by the following relation:

$$149 \quad RSR = \frac{\sqrt{\sum_{i=1}^N (I_m(t_i) - I_s(t_i))^2}}{\sqrt{\sum_{i=1}^N (I_m(t_i) - \bar{I}_m)^2}}, \quad (6)$$

150 where  $N$  is the number of simulated and measured infiltration depths and  $t$  is time (s).

151 Following the procedure explained above, the field equivalent sorptivity and the saturated  
 152 hydraulic conductivity were determined once per year at each surveyed farm. These estimated field-  
 153 equivalent parameters were used to calculate the advance-infiltration profiles for each irrigation  
 154 event performed by the farmers and monitored within the study period.

155 Each saturated hydraulic conductivity value estimated using the proposed approach was compared  
 156 to three values of saturated hydraulic conductivity estimated by BEST tests performed at the same  
 157 location where the soil samples were collected, as explained in section 2.3. For the sake of  
 158 comparison, the  $K_S$  values were also determined by seven pedotransfer functions based on particle  
 159 size distribution data and  $\theta_s$  (namely, Brakensiek et al., 1984; Cosby et al., 1984; Puckett et al.,  
 160 1985; Saxton et al., 1986; Campbell and Shiozawa, 1994; Dane and Puckett, 1994; Ferrer-Julìà et  
 161 al., 2004).

## 162 *2.2 Verification of the assumption of short irrigation duration*

163 According to the limitations of the advance-infiltration model proposed by Philip and Farrell (1964)  
 164 for predicting long-term infiltration processes, the short irrigation duration assumption has to be  
 165 verified to employ this advance-infiltration model. In the proposed approach, the verification of the  
 166 assumption is performed according to the methodology proposed by Knight (1980), which requires  
 167 three variables. The first is a dimensionless time variable defined as:

$$168 \quad \tau_k = K_S^2 t / S^2. \quad (7)$$

169 The second is a dimensionless variable for the head on the soil surface given by:

$$170 \quad C_k = K_S h_{surf} / S^2, \quad (8)$$

171 where,  $h_{surf}$  (L) is the water head imposed on the field surface during the irrigation process.



172 The third is a dimensionless advancement variable given by the “linear” soil function proposed by  
 173 Philip (1966, 1969), which, at small times, is given by the following equation when  $C \neq 0$ :

$$174 \quad x_k = \frac{\tau}{C_k} - \frac{2\tau^{3/2}}{3C_k^2} - \frac{(2C_k - \pi)\tau^2}{8C_k} - \frac{(2C_k^2 - 4C_k\pi + \pi^2)\tau^{5/2}}{15\pi C_k^4}. \quad (9)$$

175 The dimensionless advancement is calculated by employing the linear soil function (Eq. 9)  
 176 proposed by Philip (1966, 1969). Both the dimensionless advancement and time variables are  
 177 compared to their maximum values ( $\tau_{max} = 1.4$  and  $x_{max} = 0.4$ ), which are the limits of the area of a  
 178  $\tau$ - $x_k$  plot for which the time can be considered short. Because the Philip and Farrell advance-  
 179 infiltration model behaves as the linear soil function, proposed by Philip (1966, 1969), for any  
 180 values of  $C_k$  within the range between 0 and 2 (Knight, 1980), the short duration assumption is  
 181 verified for  $\tau_k$  and  $x_k$  values lower than  $\tau_{max}$  and  $x_{max}$ , respectively.

### 182 2.3 Saturated hydraulic conductivity validation

183 In this study, the BEST infiltration test (Lassabatère et al., 2006) was employed to obtain an  
 184 estimation of  $K_S$  that is independent from the advance-infiltration model and the soil water content  
 185 measured by the TDR station. These independent values of  $K_S$  were determined once a year at the  
 186 same locations where the soil samples were collected. They were compared to the  $K_{Seq}$  values  
 187 estimated following the methodology presented in section 2.1 to validate the latter.

188 In the BEST procedure, the scale parameter for the residual water content ( $\theta_r$ ) was assumed to be  
 189 zero, and the initial soil water content and the soil water content at field saturation ( $\theta_S$ ) were  
 190 estimated using the TDR measurements collected before and after the infiltration tests. The values  
 191 of  $K_S$  and  $S$  were determined by fitting the experimental infiltration data to the set of equations  
 192 proposed by Lassabatère et al. (2006). Finally, the scale parameter for the matric potential ( $h_g$ ) for  
 193 the water retention curve of van Genuchten (1980) was obtained using Eq. (5).

### 194 2.4 Farm descriptions

195 Three farms, characterized by their analogous soil conditions were selected as testing sites. All  
 196 farms performed border irrigation on corn (*Zea mays* L.) crops. These farms are located in the

197 Cuneo district (namely: farm 1, Ceresole d'Alba, Lat. 44° 48' 37", Lon. 7° 46' 45"; farm 2,  
198 Fossano, Lat. 44° 34' 40", Lon. 7° 42' 06"; farm 3, Sommariva del Bosco, Lat. 44° 44' 21", Lon. 7°  
199 43' 33") in north-western Italy. The soil of the three farms, were analysed according to the USDA  
200 Keys to Soil Taxonomy (Soil Survey Staff, 2010), and belong to the following families: farm 1,  
201 Fluventic Dystrudept, coarse-loamy, mixed, nonacid, mesic; farm 2, Acquic Haplustept, coarse-  
202 loamy over loamy-skeletal, mixed, nonacid, mesic; farm 3, Acquic Haplustept, loamy-  
203 skeletal,mixed,nonacid,mesic.

204 Despite the fact that the soils belonged to similar textural classes (i.e., loam and silty loam), the  
205 soils exhibited differences in their hydraulic properties (e.g., the soil water content at saturation  
206 conditions and the field capacity, listed in Table 1) primarily because of the differences in tillage  
207 practices and the varying percentages of stones in the fields. The percentages of sand, clay, and silt  
208 (defined according to the USDA Classification System (Soil Survey Laboratory Staff, 1992)) are  
209 included in Table 2 and were calculated from the average of the laboratory analysis of four samples  
210 collected at four different depths (between 0.05 m and 0.6 m). The percentages of stones were  
211 determined from the analysis of two vertical soil profiles for each field. These analyses were  
212 performed during the 2007 irrigation season.

213 During the three-year period (2006-2008), the farmers executed thirty irrigation events, and fifteen  
214 were monitored with specific measurement campaigns. In such a period, the border sizes of these  
215 farms changed (Table 3) because the farmers autonomously followed their normal habits regarding  
216 cultivation management and irrigation practices. However, the practices of the farmers are crucial  
217 for the study because monitoring real-world agriculture was one of the study's main objectives. All  
218 farmers cultivated the corn (*Zea mays* L.) on bays composed by multiple rows (10 rows per bay at  
219 farm 1, 13 rows per bay at farm 2, and 8 rows per bay at farm 3) with interrow spacing of 0.75 m.  
220 The rows were oriented along the maximum field length. At the end of the field a small canal to  
221 collect surface runoff was seasonally dug.

## 222 2.5 TDR stations

223 Time Domain Reflectometry is a well-known technique that is commonly accepted for the  
224 assessment of water content and other physical properties of porous media by permittivity  
225 measurements (Topp et al., 1980; Robinson et al., 2003; Canone et al., 2009; Baudena et al., 2012;  
226 Previati et al., 2012). Soil permittivity measurements were carried out using a device composed by  
227 one TDR cable tester (Tektronix Metallic Cable Tester 1502C manufactured by Tektronix Inc.,  
228 Beaverton, OR, USA) connected to a notebook and a multiplexer. The system allowed automatic  
229 measurements of soil permittivity at eight points along the soil profile. The TDR signals were  
230 sampled and acquired using the WinTDR software (Or et al., 2004) and stored in the hard disk of a  
231 notebook. The soil bulk permittivity was monitored from the beginning to the end of the irrigation  
232 events at a time interval of 3 minutes, and the volumetric soil water content was computed using the  
233 composite dielectric approach described by Roth et al. (1990).

234 The installed TDR probes were 150 mm long and were composed of three stainless steel rods held  
235 together by a nylon spacer. All of the probes were calibrated according to the method proposed by  
236 Heimovaara (1993). All of the connections were made using RG58 50  $\Omega$  coaxial cables. Each of the  
237 10 probes was horizontally inserted into the soil. The probes were arranged in two vertical profiles  
238 at the depths of 0.05 m, 0.15 m, 0.30 m, 0.45 m, and 0.65 m to monitor the entire root zone. In one  
239 of the fifteen examined cases, a layer of stones prevented the 0.65 m depth measurement (Fig. 1).  
240 The TDR stations were located at approximately one-third of the field length along a bay situated at  
241 the centre of the field.

242 Each volumetric water content measurement was then associated with and weighted in relation to its  
243 specific corresponding volume of soil (equivalent to the thickness of each monitored layer). In other  
244 words, the value obtained by the probe placed at a depth of 0.05 m was considered representative of  
245 the soil layer between 0 m and 0.10 m depth, whilst the soil water content value obtained by the  
246 0.15 m depth probe was considered representative of the soil layer between 0.10 m and 0.225 m of  
247 depth, and thus forth for the deeper probes. Thus, the volumes of water that infiltrated the soil and

248 the evolution of the water content profiles over time during the irrigation process (Fig. 2) were  
249 obtained for the three farms.

## 250 *2.6 The measurements of irrigation parameters*

251 Field measurements were performed to acquire the following data for each monitored irrigation  
252 event: i) the duration of the irrigation event,  $t_{ir}$  (T); ii) the irrigation inflow rate,  $F_r$  ( $L^3 T^{-1}$ ); iii) the  
253 volume of water delivered during the irrigation event,  $V_d$  ( $L^3$ ), and average volume of water  
254 delivered per unit area, ( $L^3 L^{-2}$ ); and iv) the water head imposed on the field surface during the  
255 irrigation event,  $h_{surf}$  (L), which was measured by a water level staff gauge (marked at every  
256 millimetre) under steady flow conditions at the upstream position. We also recorded the occurrence  
257 of surface runoff, the time at which the surface runoff was eventually starting. The volume of  
258 surface runoff and deep percolation were not measured. They were calculated from the partition of  
259 the applied water volume determined from infiltration profiles as explained in the following section.  
260 Furthermore, the number of irrigation events initiated during the season by each farmer, the  
261 irrigation parameters and the infiltration advance profiles were used to partition the applied water  
262 volumes.

## 263 *2.7 Partitioning of the applied water volume*

264 The volume of storable water at field capacity  $V_{fc}$  ( $L^3$ ) was calculated by multiplying the water  
265 content at field capacity by the volume of soil in the root layer. The soil water content at field  
266 capacity was calculated as the soil water content value given by the van Genuchten (1980) equation  
267 for the matric potential value of -3.3 m. Using the infiltration advance profiles and the scheme given  
268 in Figure 3, the volume of water applied to the field was partitioned as follows: i) the total volume  
269 of water stored in the soil  $V_{st}$  ( $L^3$ ), which was calculated by subtracting the water volume lost  
270 through deep percolation from the total infiltrated volume and then adding the volume stored on the  
271 surface; ii) the volume stored at the surface  $V_s$  ( $L^3$ ), which is the volume of water on the surface of  
272 the field after the completion of the water application; iii) the volume of water lost by surface runoff

273  $V_r$  ( $L^3$ ), which was calculated as the sum of the infiltrated water volume and the volume of water  
274 stored on the land surface beyond the end of the field (when the irrigation ended); and iv) the  
275 volume lost through deep percolation below the root layer  $V_{dp}$  ( $L^3$ ). The volume of water stored on  
276 the surface ( $V_s$ ) was divided into two parts. The amount of the  $V_s$  that remained on the portion of the  
277 field where deep percolation occurred was considered lost. The remaining volume was added to the  
278 stored volume. The errors introduced by such assumptions are small because  $V_s$  never exceeded  
279 10% of the stored volume (Table 4).

280 The volumes of water lost by surface runoff and deep percolation were not measured. They were  
281 calculated from the infiltration profiles given by the infiltration advance model. Considering that the  
282 model was validated on the infiltrated water depth at the locations of the TDR stations (as shown in  
283 section 3.1) and the aim of the work was to employ simple measurement techniques, we choose not  
284 to measure the volume of water lost by runoff and deep percolation. Such measurements were not  
285 necessary for the validation of the model and their acquisition would have severely complicated the  
286 field measurement campaigns.

287 All calculated water volumes were used to compute the application efficiency ( $E_a$ ), the storage  
288 efficiency ( $E_s$ ), and the distribution efficiency ( $E_d$ ) terms for the field-equivalent parameters. For  
289 further comparison, the efficiency terms were also calculated for the three sets of parameters  
290 determined by the infiltration BEST tests. Finally, the proposed model was used to simulate the  
291 effects of changes in various irrigation parameters, namely, the flow rate ( $F_r$ ), the irrigation event  
292 duration ( $t_{ir}$ ), the volume of water delivered ( $V_d$ ) and the initial soil moisture  $\theta_i$ .

### 293 *2.8 Irrigation efficiencies*

294 The application efficiency ( $E_a$ ) quantifies the volume of water actually stored in the root layer in  
295 relation to the volume of water delivered. The storage efficiency ( $E_s$ ) quantifies the recovery of the  
296 field water deficit. The distribution efficiency ( $E_d$ ) quantifies the homogeneity of water storage  
297 along the field. The combination of these three efficiency terms provides the global efficiency of the

298 irrigation process. Additionally, by employing the proposed method, the choice of the best irrigation  
299 practice may be achieved.

300 The water application and storage efficiencies are given according to the relationships proposed by  
301 Kruse et al. (1990):

$$302 \quad E_a = \frac{V_{st}}{V_d}, \quad (10)$$

$$303 \quad E_s = \frac{V_{st}}{V_{fc}}, \quad (11)$$

304 The distribution efficiency is determined using the relationship proposed by Burt et al. (1997):

$$305 \quad E_d = \frac{V_{lq}}{V_{fq}}, \quad (12)$$

306 where,  $V_{lq}$  is the volume of water stored in the last quarter of the field ( $L^3$ ), whilst  $V_{fq}$  is the volume  
307 stored in the first quarter of the field ( $L^3$ ).

## 308 *2.9 Predictive simulations*

309 After the irrigation efficiencies of the monitored events were calculated, and the model was  
310 employed to predict the irrigation efficiencies of simulated irrigation events. In particular, the  
311 irrigation simulations were performed using seven different combinations of the irrigation  
312 parameters (i.e.,  $V_d$ ,  $F_r$  and  $\theta_i$ ) to determine their influence on irrigation efficiency. The values of  
313 the irrigation parameters are presented and discussed in section 3.4.

## 314 **3 Results and Discussion**

### 315 *3.1 Model validation*

316 The first step of the model validation was the confirmation of the short duration assumption. For the  
317 measured irrigation times used in this study, the calculated values of  $x_k$  and  $\tau_k$ , as proposed by  
318 Knight (1980), corresponded to a short-duration behaviour. These parameter values are given in  
319 Table 5. The dimensionless time and advancement variables never exceeded the maximum values  
320 ( $\tau_{max} = 1.4$  and  $x_{max} = 0.4$ ) proposed by Knight (1980). According to Knight (1980), employing this

321 combination of values ensures that the behaviour of the Philip and Farrell analytical solution  
322 matches the actual advance-infiltration processes.

323 Using the proposed method, the field-equivalent saturated conductivity ( $K_{Seq}$ ) values, obtained by  
324 fitting of Eqs. (1,2 and 5) as explained in section 2.1, were close to the three sets of values  
325 estimated by the BEST infiltration tests (Tables 6 and 7). The differences among the  $K_{Seq}$  values and  
326 the results of the corresponding BEST tests were almost always lower than 16% of the  $K_S$  values  
327 obtained from BEST tests. Only two differences exceeded that range. Both values were recorded at  
328 Farm 2, one in the year 2007 (36.7%) and the other in the year 2008 (-40.9%), as shown in Table 7.  
329 The results of the BEST tests indicated low  $K_S$  variability across the fields of Farm 1 and Farm 3, as  
330 shown by the standard deviation of  $K_S$  values (Table 6) and by the three  $K_S$  values measured at each  
331 field, and among the three-year period (Table 7). The low variability of  $K_S$  was probably attributed  
332 to the tillage practices: each year, the soil structure was effectively destroyed by the rototilling  
333 practices performed prior to sowing. In any case, for further comparison, the root mean square error  
334 (RMSE) between the results of seven different pedotransfer functions applied for the estimation of  
335  $K_S$  and the  $K_{Seq}$  values were evaluated. The RMSE between the results of the BEST tests and the  
336  $K_{Seq}$  values were also evaluated. The  $K_S$  values are depicted in Figure 4 and the RMSE are listed in  
337 Table 8. Only one of the seven pedotransfer functions (Puckett et al., 1985) produced results that  
338 are in agreement with the estimated  $K_{Seq}$  values.

339 The infiltration depths of water were then compared with the infiltration profiles, which were  
340 calculated using the fitted  $K_{Seq}$  values (Table 6), the  $K_S$  values obtained by the BEST tests, and the  
341 irrigation parameters chosen by the farmers. The infiltration depths were obtained from the TDR  
342 soil water content measurements. Finally, the differences between the infiltration profiles and the  
343 infiltrated depth of water were assessed. The infiltration model outputs were always in good  
344 agreement with the measured infiltration depths (Fig. 5), as shown by the differences between  
345 simulated and measured infiltration depths reported in Table 9. The highest and the lowest  
346 differences recorded during the fifteen monitored events were 0.018 m and 0.002 m. The SRS

347 calculated to evaluate the performance of the proposed method on the monitored irrigation events  
348 was 0.22 at Farm 1, 0.07 at Farm 2 and 0.05 at Farm 3. Cook et al. (2013) found SRS values  
349 between 0.29 and 6.83 for the Philip and Farrel (1964) infiltration-advance solution for short-term  
350 duration. The low SRS obtained in our experiments is due to the direct measurement of the  
351 infiltration depth. Cook et al. (2013) employed infiltration depths estimated by Taylor (1981) using  
352 the mass balance method of Finkel and Nir (1960). The highest difference between the simulated  
353 and measured data observed during the first irrigation event performed by farm 1 in 2007 was 0.013  
354 m. This difference was recorded at a station located 30 m from the beginning of the field at 720 s  
355 and 913 s ( $t_{ir}$ ) after the start of irrigation. The simulated infiltration depths were 0.178 m and 0.203  
356 m, respectively, and the measured depths were 0.191 m and 0.216 m, respectively. The minimum  
357 difference occurred during the same irrigation event, was recorded at 360 s after the start of  
358 irrigation, at a station located 32 m from the beginning of the field. The simulated infiltration depth  
359 was 0.116 m and the measured depth was 0.114.

### 360 *3.2 Irrigation efficiencies vs. hydraulic parameters*

361 As expected from Eqs. 1, 2 and 5, the analysis of the influence of the initial water content on the  
362 volume of water that might infiltrate the soil demonstrates the relationship between  $\theta_i$  and the  
363 irrigation efficiency. The analysis of irrigation events performed at the constant values of  $K_S$  and  $F_l$ ,  
364 and similar values of  $F_r$ , indicate that a high  $\theta_i$  results in low  $E_a$  values because of the low  
365 infiltration rate and, consequently, high surface runoff. Moreover, high  $\theta_i$  values indicate a low soil  
366 retention capacity, which results in deep percolation losses even during low infiltration events.

367 The  $K_{Seq}$  values and the three  $K_S$  values estimated by the BEST infiltration tests were used to  
368 calculate four sets of efficiency values. The analysis of the application and storage efficiency values  
369 indicates that  $K_S$  has only a minor influence on the results (Figs. 6a and 6b) because the variability  
370 in  $K_S$  was very low. The low variability in  $K_S$  values could only transform deep percolation losses  
371 into runoff losses when there was little change in the volume of water stored in the root layer. Thus,



372 the distribution efficiency is more highly influenced by  $K_S$  than the other two efficiencies (Fig. 6c)  
373 because it depends on the shape of the infiltration profile and can be modified by small variations in  
374  $K_S$ . The variation among the  $E_a$  values of the irrigation events was negligible (below 0.05) in almost  
375 all cases. As indicated in Figure 6a, we observed the highest variation of  $E_a$  in the first irrigation  
376 performed on farm 3 in 2006 (0.06). The variation among the  $E_s$  values was also negligible in  
377 almost all cases; the highest value was also observed for the first irrigation performed on farm 3 in  
378 2006 (0.07), as shown in Figure 6b. The variation among  $E_d$  values was negligible for six of the  
379 fifteen irrigation events monitored; the highest  $E_d$  value was again observed for the first irrigation  
380 performed on farm 3 in 2006, as shown in Figure 6c, but this value was much higher (0.27) than the  
381 values found for  $E_a$  and  $E_s$ .

### 382 *3.3 Irrigation efficiencies vs. irrigation parameters*

383 The irrigation parameters varied considerably during the study period. In fact, the farmers were  
384 completely free to manage the irrigation events. Relying on their experience and on an empirical  
385 evaluation of the soil water content, many farmers tried to limit the effect of the initial water content  
386 by varying the volume of irrigation water and, in several cases, the flow rate (Table 10). Because of  
387 farm management needs, the farmers also changed the lengths of several plots during the three-year  
388 period.

389 The variations in the lengths of the plots, combined with a non-proportional variation in the flow  
390 rate and the temporal variability of the field-scale saturated hydraulic conductivity, resulted in  
391 variations in the time required for the water to reach the end of the field ( $t_{fl}$ ). Additionally, this  
392 variation caused i) a modification of the time required to impose a uniform hydraulic head over the  
393 entire field surface and ii) a change in the volume of infiltrated water that, in some cases, was large  
394 enough to mask the effects of the initial water content. To limit the effects of the farmers' choices  
395 and to assess the real influence of  $t_{fl}$  and  $\theta_i$  on irrigation efficiency, the analysis was conducted on  
396 pairs of irrigation events in which the other parameters were maintained nearly as constants.

397 As indicated in Eqs. (1) and (5), the analysis of irrigation events performed with constant values of  
398  $K_S$  and  $F_l$  and similar values of  $F_r$  indicate that the effect of  $t_{fl}$  on irrigation efficiency is inversely  
399 proportional to  $\theta_i$ . High  $\theta_i$  values are associated with low  $t_{fl}$  values, which result in low  $E_a$  values  
400 because of the high surface runoff. Low  $t_{fl}$  values are associated with the rapid imposition of a  
401 constant head over the bay, which causes high values of  $E_s$  and  $E_d$  (Figs. 6b, 6c). Only a few  
402 exceptions were found. In the examined pairs of irrigation events, the exceptions were explained by  
403 the differences in  $t_{ir}$  and  $F_r$  employed by the farmers.

404 By employing higher flow rates, each of the farms achieved higher distribution efficiency values.  
405 However, because of the surface runoff, the benefits of a higher  $E_d$  often did not compensate for the  
406 decrease in the application efficiency values. The irrigation time ( $t_{ir}$ ) cannot be decrease to approach  
407  $t_{fl}$  to avoid surface runoff because a low  $t_{ir}$  would cause a great difference in the time of infiltration  
408 between upstream and downstream areas, which would strongly reduce the distribution efficiency  
409 values. The best compromise was often achieved by modifying the flow rate. However, if the  
410 irrigation district is provided with a network of gully channels, the volumes of water lost as surface  
411 runoff should not be counted among the losses that affect the application efficiency (Clemmens et  
412 al., 2008).

413 In most cases, the volumes of water stored during the monitored irrigation events balanced the  
414 hydraulic deficit of the root layer. However, whilst the irrigations performed at farm 1 resulted in  
415 water storage efficiencies that were significantly lower than one, all of the irrigations performed at  
416 farm 2 and 3 resulted in higher  $E_s$  values, but with the disadvantage of high deep-percolation losses.

### 417 *3.4 Scenario analysis and considerations for predictive settings*

418 The infiltration profile across the entire field, which was simulated using the actual parameters of  
419 the first irrigation event that was performed at farm 1 in 2007 (Fig. 7a), was compared with the  
420 infiltration profiles produced by seven irrigation simulations. In the first three cases (Figs. 7b to 7d),  
421 the duration of the irrigation event and the flow rates were altered. The infiltration profiles

422 described by cases 4-7 (Fig. 7e to 7h) were produced with differing flow rates and initial water  
423 contents. The values of the input parameters employed in the simulations are summarized in Table  
424 11 in addition to the simulation results.

425 In the first case (Fig. 7b), the flow rate was reduced to a value of  $0.04 \text{ (m}^3 \text{ s}^{-1}\text{)}$ , whilst the duration  
426 of the irrigation event was increased by approximately one-third (1200 s) (Table 11). In this case, an  
427  $E_a$  value of 0.95 was achieved because the water flowed only slightly past the end of the field and  
428 slightly deeper than the bottom of the soil root layer; hence, there were only small amounts of  
429 surface runoff and percolation losses. Although the watering volume of this first case was greater  
430 than that of the real monitored case, the majority of the water was stored equally and the  $E_s$  was  
431 slightly improved because of this level of storage. In contrast, there was a reduction in  $E_d$  that  
432 caused a reduction in the overall irrigation efficiency.

433 In the second case (Fig. 7c), the flow rate was equal to the previous case (Table 11), but the  
434 duration of the irrigation event was increased by one-third (1600 s). The results indicate an  
435 improvement in the  $E_s$  and  $E_d$  and a decrease in the  $E_a$  value. The watering volume considered in  
436 this case was higher than the two previous cases, which suggests that the necessary watering  
437 volume was surely underestimated for the monitored case.

438 In the third case (Fig. 7d), the flow rate was the same as in the real irrigation event, whilst the event  
439 duration was the same as in the second case, thus applying a watering volume that was almost twice  
440 as large as the volume of the real irrigation event. In this case, both the  $E_s$  and  $E_d$  increased to a  
441 value of 1, but the  $E_a$  value (0.64) was the lowest among all of the cases considered (Table 11).

442 In the fourth case (Fig. 7e), the flow rate was increased to a value of  $0.06 \text{ (m}^3 \text{ s}^{-1}\text{)}$  but the irrigation  
443 duration was maintained at the actual value used by the farmer (Table 11). Compared to the real  
444 irrigation event, the results indicate an increase in the  $E_s$  (+0.04) and  $E_d$  (+0.10) and a decrease in  
445 the  $E_a$  (-0.11). The  $E_a$  value was comparable to the value obtained in the second case, but the  $E_s$  and  
446  $E_d$  values were lower.

447 In the fifth case (Fig. 7f), the flow rate was increased to a value of  $0.07 \text{ (m}^3 \text{ s}^{-1}\text{)}$ , whilst the irrigation  
448 event duration was maintained at the actual irrigation duration. Compared to the previous case, the  
449  $E_s$  and  $E_d$  increased slightly ( $+0.02$  and  $+0.07$ , respectively). In this case, the  $E_a$  value was slightly  
450 lower than in the second case, whilst the storage efficiency value decreased by  $0.12$ .

451 In the sixth case (Fig. 7 g), the flow rate and the irrigation event duration values were the same as  
452 the values from the real irrigation event (Table 11), but the initial soil water content was set to a  
453 value of  $0.05 \text{ (m}^3 \text{ m}^{-3}\text{)}$ , which is lower than the measured value. Compared to the real event, the  
454 results suggest an increase in the  $E_a$  ( $+0.05$ ) because of the higher infiltration rate caused by the  
455 high value of the matric potential, which is inversely proportional to the soil water content.

456 When compared to the real irrigation event, the results of the first six cases also indicate a reduction  
457 in the  $E_s$  because the water deficit was higher in these simulations. Additionally, the results  
458 demonstrate a reduction in the  $E_d$  because of the difference in the depth of water infiltration at the  
459 beginning and at the end of the field during the time required to establish a uniform hydraulic head  
460 over the field. The simulation results suggest that, when the irrigation is performed at a  $\theta_i$  that is  
461 lower than in the actual irrigation event considered, the flow rate should be increased.

462 Finally, in the seventh simulation (Fig. 7 h), the initial water content was assumed to be higher than  
463 the real value and was set to a value of  $0.15 \text{ (m}^3 \text{ m}^{-3}\text{)}$ . However, the other parameters were the same  
464 as in the real irrigation event (Table 11). As expected, the results were the opposite of the previous  
465 case. Compared to the real event, the  $E_a$  decreased ( $-0.06$ ) and both the  $E_s$  and  $E_d$  increased to  $+0.12$   
466 and  $+0.10$ , respectively.

467 According to the simulation results, the best  $E_a$  value was obtained for the sixth case, but the  
468 corresponding  $E_s$  and  $E_d$  values were the lowest. This result suggests that this choice would  
469 represent a misuse of water. In contrast, the best  $E_s$  and  $E_d$  values were registered in the third case,  
470 but the  $E_a$  value was the lowest. The real irrigation event considered represents a compromise  
471 between saving water and the best use of water for crop production. The second case is also a good  
472 compromise because a slightly greater volume of water is employed to obtain a large increase in  $E_s$

473 and  $E_d$ . A higher flow rate was not always the best solution. A comparison between the results of  
474 the fourth and fifth cases indicates that a high flow rate could be employed to increase the  $E_s$  and  $E_d$   
475 values. However, this solution can only be applied in cases where the irrigation district is provided  
476 with a network of gully channels to avoid surface runoff losses and maintain high values of  $E_d$ .  
477 For the monitored irrigation events, the flow rate employed by the farmer was suitable for the field  
478 conditions, whereas the watering volume was insufficient, as shown in the third simulation (Fig.  
479 7d). Similar to the previous simulations, the sixth and seventh simulations (Fig. 7 g and 7 h)  
480 demonstrated the influence of the initial field conditions. These results suggest that farmers should  
481 apply larger watering volumes, but less frequently, to obtain higher irrigation efficiencies.  
482 Moreover, to avoid low  $E_s$  and  $E_d$  values, irrigation should not be performed when the soil water  
483 content is too low.

## 484 **5 Conclusions**

485 In this study, a method based on the Philip and Farrel (1964) advance-infiltration model was  
486 proposed for i) calculating the border irrigation efficiency from four simple field measurements  
487 (inflow rates, irrigation durations, and soil water content values monitored at only one point of the  
488 field at the beginning and at the end of the irrigation processes) and ii) for testing the sensitivity of  
489 irrigation efficiency to surface irrigation operational parameters.

490 The irrigation efficiency of 15 real irrigation events performed on three different farms during the  
491 growing seasons in 2006, 2007 and 2008 were analysed. Finally, a scenario analysis based on data  
492 collected during one of the surveyed events was also performed by altering the irrigation parameters  
493 that affect irrigation efficiency (namely, irrigation duration, flow rate, and initial soil water content).  
494 The proposed method proved to be capable of describing real irrigation practices. Moreover, the  
495 method was capable of evaluating the changes in irrigation efficiency as a consequence of  
496 variations in the operational irrigation parameters.

497 The results demonstrate that the equivalent saturated hydraulic conductivities estimated using the  
498 proposed method is always in good agreement with the  $K_S$  values estimated using the infiltration  
499 tests performed at three different positions in each field. Additionally, the irrigation efficiencies  
500 calculated using both the proposed approach and using the parameters estimated by infiltration  
501 measurements were in good agreement.

502 The efficiencies analysis (of the water application, storage, and distribution efficiencies) highlighted  
503 the marked variability in the values among the monitored farms and within each farm. This level of  
504 variability was associated with the variations in the watering volumes and flow rates. The influence  
505 of the initial soil water content on the storage efficiency was clear, but some exceptions were  
506 observed when irrigation durations was sufficiently long to mask the effects of the initial soil water  
507 content.

508 The analysis of both the simulated scenarios and fifteen monitored irrigation events demonstrated  
509 the need to irrigate these fields using lower flow rates and higher irrigation durations than those  
510 currently used by the farmers. The scenario analysis also revealed that the irrigation efficiencies are  
511 highly dependent on the initial soil water content.

## 512 **6 Acknowledgements**

513 This study was partially funded by the Italian Ministry of Research through Italian Research Project  
514 of Relevant Interest (PRIN2010-2011), prot. 20104ALME4, “National network for monitoring,  
515 modeling, and sustainable management of erosion processes in agricultural land and hilly-  
516 mountainous area” (PI Mario Aristide Lenzi) and through the project PRIN2010-11 “New  
517 methodologies for water resources management in hydro-climatic uncertainty scenarios” (PI  
518 Alberto Bellin).

519 Special thanks are given to all of the staff of the Coldiretti Cuneo, to the farmers for their endless  
520 patience and to Prof. Randel Haverkamp for his helpful suggestions.

## 521 **7 References**

522 Arnell, N.W., 1999. Climate change and global water resources. *Global Environ. Change* 9, S31-  
523 S49.

524 Bagarello, V., Di Prima, S., Iovino, M., Provenzano, G., Sgroi, A., 2011. Testing different  
525 approaches to characterize Burundian soils by the BEST procedure. *Geoderma* 162, 141-150.

526 Baudena, M., Bevilacqua, I., Canone, D., Ferraris, S., Previati, M., Provenzale, A., 2012. Soil water  
527 dynamics at a midlatitude test site: Field measurements and box modeling approaches. *J. Hydrol.*  
528 414-415, 329-340. doi: 10.1016/j.jhydrol.2011.11.009

529 Bautista, E., Clemmens, A.J., Strelkoff, T.S., 2009. Structured Application of the Two-Point  
530 Method for the Estimation of Infiltration Parameters in Surface Irrigation. *J. Irrig. Drain. Eng.*  
531 135(5), 566–578.

532 Brakensiek, D.L., Rawls, W.J., Stephenson, G.R., 1984. Modifying SCS hydrologic soil groups and  
533 curve numbers for rangeland soils. ASAE Paper No. PNR-84-203, St. Joseph, MI.

534 Brooks, R.H., Corey, A.T., 1964. Hydraulic properties of porous media. *Hydrology Paper* 3,  
535 Colorado State University, Fort Collins, CO, USA.

536 Burt, C.M., Clemmens, A.J., Strelkoff, T.S., Solomon, K.H., Bliesner, R.D., Hardy, L.A., Howell,  
537 T.A., Eisenhauer, D.E., 1997. Irrigation Performance Measures: Efficiency and Uniformity. *J.*  
538 *Irrig. Drain. E-ASCE* 123(6), 423-442. doi:10.1061/(ASCE)0733-9437(1997)123:6(423)

539 Campbell, G.S., Shiozawa, S., 1994. Prediction of hydraulic properties of soils using particle-size  
540 distribution and bulk density data. In: van Genuchten, M.T., Leij, F.J., Lund, L.J. (Eds.),  
541 *Proceedings of the International Workshop on Indirect Methods for Estimating the Hydraulic*  
542 *Properties of Unsaturated Soils*, University of California, Riverside, CA, pp. 317-328.

543 Canone, D., Previati, M., Ferraris, S., Haverkamp, R., 2009. A New Coaxial Time Domain  
544 Reflectometry Probe for Water Content Measurement in Forest Floor Litter. *Vadose Zone J.* 8,  
545 363-372.

546 Canone, D., Ferraris, S., Sander, G., Haverkamp, R., 2008. Interpretation of water retention field  
547 measurements in relation to hysteresis phenomena. *Water Resour. Res.* 44, W00D12. doi:  
548 10.1029/2008WR007068

549 Chohin-Kuper, A., Rieu, T., Montginoul, M., 2003. Water Policy Reforms: Pricing Water, Cost  
550 Recovery, Water Demand and Impact on Agriculture. Lessons from the Mediterranean  
551 experience, at the water pricing seminar, June/July 2003, Agencia Catalana del Agua and World  
552 Bank Institute, Barcelona. [http://www.emwis.net/documents/database/water-policy-reforms-](http://www.emwis.net/documents/database/water-policy-reforms-pricing-water-cost-recovery)  
553 [pricing-water-cost-recovery](http://www.emwis.net/documents/database/water-policy-reforms-pricing-water-cost-recovery). Last checked 25/09/2013.

554 Clemmens, A.J., Allen, R.G., Burt, C.M., 2008. Technical concepts related to conservation of  
555 irrigation and rain water in agricultural systems. *Water Resour. Res.* 44, W00E03. doi:  
556 10.1029/2007WR006095

557 Collis-George, N., Freebairn, D.M., 1979. A laboratory and field study of border check irrigation.  
558 *Aust. J. Soil Res.* 17, 75-87.

559 Cook, F.J., Knight, J.H., Doble, R.C., Raine, S.R., 2013. An improved solution for the infiltration  
560 advance problem in irrigation hydraulics. *Irrig. Sci.* 31, 1113-1123.

561 Cosby, B.J., Hornberger, G.M., Clapp, R.B., Ginn, T.R., 1984. A statistical exploration of the  
562 relationship of soil moisture characteristics to the physical properties of soils. *Water Resour.*  
563 *Res.* 20 (6), 682-690.

564 Dane, J.H., Puckett, W., 1994. Field soil hydraulic properties based on physical and mineralogical  
565 information. In: van Genuchten, M.T., Leij, F.J., Lund, L.J. (Eds.), *Proceedings of the*  
566 *International Workshop on Indirect Methods for Estimating the Hydraulic Properties of*  
567 *Unsaturated Soils*, University of California, Riverside, CA, pp.389-403

568 Fereres, E., Soriano, M.A., 2007. Deficit irrigation for reducing agricultural water use. *J. Exp. Bot.*  
569 58, 147–159.



570 Ferraris, S., Bevilacqua, I., Canone, D., Pognant, D., Previati, M., 2012. The finite volume  
571 formulation for 2-D second-order elliptic problems with discontinuous diffusion/dispersion  
572 coefficients. *Math. Probl. Eng.* 2012, 1-23. doi: 10.1155/2012/187634

573 Ferrer-Julià, M., Estrela Monreal, T., Sánchez del Corral Jiménez, A., García Meléndez, E., 2004.  
574 Constructing a saturated hydraulic conductivity map of Spain using pedotransfer functions and  
575 spatial prediction. *Geoderma* 123, 275-277.

576 Finkel, H.J., Nir, D., 1960. Determining infiltration rates in an irrigation border. *J. Geophysical Res.*  
577 65(7), 2125-2131.

578 Gandolfi, C., Savi, F., 2000. A Mathematical Model for the Coupled Simulation of Surface Runoff  
579 and Infiltration. *J. Agr. Eng. Res.* 75, 49-55.

580 Haverkamp, R., Kutilek, M., Parlange, J.-Y., Rendon, L., Krejka, M., 1988. Infiltration under  
581 ponded condition: 2. Infiltration equation tested for parameter time dependence and predictive  
582 use. *Soil Sci.* 145, 317-329.

583 Haverkamp, R., Nimmo, J.R., Reggiani, P., 2002. Property-Transfer Models. In: Dane, J., Topp,  
584 G.C. (Eds.), *Methods of Soil Analysis, Vol.4: Physical Methods*. Soil Science Society of  
585 America, Madison, Wisconsin.

586 Haverkamp, R., Debionne, S., Viallet, P., Angulo-Jaramillo, R., Decondappa, D., 2006. Movement  
587 of moisture in the unsaturated zone. In: Delleur, J.W. (Ed.), *Groundwater Engineering*  
588 *Handbook*. 2nd ed., CRC Press LLC, Boca Raton, Florida.

589 Heimovaara, T.J., 1993. Design of triple wire Time Domain Reflectometry probes in practice and  
590 theory. *Soil Sci. Soc. Am. J.* 57,1410-1417.

591 Inglesias, A., Garrote, L., Flores, F., Moneo, M., 2007. Challenges to Manage the Risk of Water  
592 Scarcity and Climate Change in the Mediterranean. *Water Resour. Manage.* 21, 775-788.

593 Knight, J.H., 1980. An improved solution for the infiltration advance problem in irrigation  
594 hydraulics. 7<sup>th</sup> Australasian hydraulics and fluids mechanics conference, Brisbane, 18-22 august  
595 1980.

596 Kruse, E.G., Bucks, D.A., von Bernuth, R.D., 1990. Comparison of irrigation systems. In: Stewart,  
597 B.A. and Nielsen, R. (Eds.), *Irrigation of agricultural crops*. ASA-CSSA-SSSA. Madison,  
598 Wisconsin.

599 Lassabatère, L., Angulo-Jaramillo, R., Soria Ugalde, J.M., Cuenca, R., Braud, I., Haverkamp, R.,  
600 2006. Beerkan Estimation of Soil Transfer Parameters Trough Infiltration Experiments - BEST.  
601 *Soil Sci. Soc. Am. J.* 70, 521-532. doi:10.2136/sssaj2005.0026

602 Lewis, M.R., Milne, W.E., 1938. Analysis of border irrigation. *Agric. Eng.* 19, 267-272.

603 Manzini, G., Ferraris, S., 2004. Mass-conservative finite volume methods on 2-D unstructured grids  
604 for the Richards' equation. *Adv. Water Resour.* 27(12), 1199-1215.  
605 doi:10.1016/j.advwatres.2004.08.008

606 Mubarak, I., Mailhol, J.C., Angulo-Jaramillo, R., Ruelle, P., Boivin, P., Khaledian, M., 2009.  
607 Temporal variability in soil hydraulic properties under drip irrigation. *Geoderma* 150, 158–165.

608 Nash, J.E., Sutcliffe, J.V., 1970. River flow forecasting through conceptual models: part 1. A  
609 discussion of principles. *J. Hydrol.* 10(3), 282-290.

610 Or, D., Silva, H. R., 1996. Prediction of surface irrigation advance using soil intake properties. *Irrig.*  
611 *Sci.* 16, 159-167.

612 Parlange, J.-Y., 1975. On solving the flow equation in unsaturated soils by optimization: Horizontal  
613 infiltration. *Soil Sci. Soc. Am. J.* 39, 415–418.

614 Philip, J.R., 1957. The theory of infiltration: 1. The infiltration equation and its solution. *Soil. Sci.*  
615 83, 345-357.

616 Philip, J.R., Farrell, D.A., 1964. General solution of the infiltration-advance problem in irrigation  
617 hydraulics. *J. Geophys. Res.* 69, 621–631.

618 Philip, J.R., 1966. A linearization technique for the study of infiltration. In: Rijtema, R.E., Wassink,  
619 H. (Eds.), *Water in the Unsaturated Zone*, Proc. UNESCO Symp. 1, 471-478.

620 Philip, J.R., 1969. Theory of infiltration. *Adv. Hydrosoci.* 5, 215-296.

621 Previati, M., Canone, D., Bevilacqua, I., Boetto, G., Pognant, D, Ferraris, 2012. Evaluation of wood  
622 degradation for timber check dams using time domain reflectometry water content  
623 measurements. *Ecol. Eng.* 44, 259-268.

624 Puckett, W.E., Dane, J.H., Hajek, B.F., 1985. Physical and mineralogical data to determine soil  
625 hydraulic properties. *Soil Sci. Soc. Am. J.* 49, 831–836.

626 Robinson, D.A., Jones, S.B., Wraith, J.M., Or, D., Friedman, S.P., 2003. A review of advances in  
627 dielectric and electrical conductivity measurements in soils using Time Domain Reflectometry.  
628 *Vadose Zone J.* 2, 444–475.

629 Roth, K., Schulin, R., Flühler, H., Attinger, W., 1990. Calibration of Time Domain Reflectometry  
630 for water content measurement using a composite dielectric approach. *Water Resour. Res.*  
631 26(10), 2267-2273.

632 Saxton, K.E., Rawls, W.J., Romberger, J.S., Papendick, R.I., 1986. Estimating generalized soil  
633 water characteristics from texture. *Soil Sci. Soc. Am. J.* 50, 1301-1036.

634 Soil Survey Laboratory Staff, 1992. Soil survey laboratory methods manual. Soil Survey  
635 Investigations Report n°42, Version 2.0. USDA-SCS U.S. Government Printing Office,  
636 Washington D.C.

637 Soil Survey Staff, 2010. Keys to Soil Taxonomy, 11th ed. USDA-Natural Resources Conservation  
638 Service, Washington, DC.

639 Strelkoff, T.S., Clemmens, A.J., Bautista, E., 2009. Estimation of soil and crop hydraulic properties.  
640 *J. Irrig. Drain. Eng.* 135(5), 537–555.

641 Taylor, A.R., 1981. A method for surface irrigation design based on infiltration using the border  
642 strip as an infiltrometer. PhD Thesis, University of Canterbury, Lincoln College, 229 pages.

643 Topp, G.C., Davis, J.L., Annan, A.P., 1980. Electromagnetic determination of soil water content:  
644 measurements in coaxial transmission lines. *Water Resour. Res.* 16 (3), 574–582.

645 van Genuchten, M.T., 1980. A closed form equation for predicting the hydraulic conductivity of  
646 unsaturated soils. *Soil Sci. Soc. Am. J.* 44, 892-898.

647 Xu, X., Kiely, G., Lewis, C., 2009. Estimation and analysis of soil hydraulic properties through  
648 infiltration experiments: comparison of BEST and DL fitting methods. *Soil Use Manage.* 25,  
649 354–361.

## 650 **FIGURE CAPTIONS**

651 **Fig. 1** Example of volumetric soil water content data collected by a TDR station with probes  
652 inserted below a row. The represented survey was performed during the first irrigation event at farm  
653 2 (in 2008). The vertical line indicates the end of the irrigation event. The 0.65 m depth data are  
654 missing because a layer of stones prevented the insertion of a TDR probe.

655 **Fig. 2** Example of soil water content profiles measured with the TDR technique every 5 minutes  
656 during the first irrigation event performed at farm 1 in 2006. The lines represent the water content  
657 profiles computed every 5 minutes from the beginning of the irrigation event,  $t_0$ , until the end of the  
658 irrigation event. The vertical axis,  $z$ , indicates the soil depth.

659 **Fig. 3** Diagram of an infiltration profile in which the whole water volume is subdivided into five  
660 portions. The horizontal black line represents the field surface, and the vertical line represents the  
661 end of the field. The data represent the real irrigation event performed on July 2008 at farm 3.

662 **Fig. 4** Comparison of the saturated hydraulic conductivity values estimated by seven different well-  
663 known pedotransfer functions and the field-equivalent values estimated by the proposed method  
664 ( $K_{s\_eq}$ ). The tested pedotransfer functions are indicated as follows: Cosby et al. (1984) = ( $K_{s\_C}$ );  
665 Saxton et al. (1986) = ( $K_{s\_S}$ ); Brakensiek et al. (1984) = ( $K_{s\_B}$ ); Ferrer-Julià et al. (2004) =  
666 ( $K_{s\_F}$ ); Campbell and Shiozawa (1994) = ( $K_{s\_CS}$ ); Puckett et al. (1985) = ( $K_{s\_P}$ ); and Dane and  
667 Puckett (1994) = ( $K_{s\_DP}$ ).

668 **Fig. 5** Soil water infiltration profiles observed during the first irrigation event performed at farm 1  
669 in 2007. The circles represent the depths of water infiltration that were measured using TDR probes.  
670 The curved lines represent the water content profiles calculated every 5 minutes from the beginning  
671 of the irrigation event ( $t_0$ ) until the end of the irrigation event ( $t_{ir}$ ). The imposed hydraulic head

672 (dash-dotted line) corresponds to the volume of water stored on the field surface divided by the total  
673 surface. The vertical axis,  $z$ , indicates the soil depth.

674 **Fig. 6** Application efficiencies ( $E_a$ ) (a), storage efficiencies ( $E_s$ ) (b) and distribution efficiencies ( $E_d$ )  
675 (c) calculated from the infiltration profiles obtained by using the field-equivalent saturated  
676 hydraulic conductivity values and the three sets of saturated hydraulic conductivity values estimated  
677 by the BEST infiltration tests. The irrigation events ( $x$  axis) are identified as farm: irrigation event:  
678 year.

679 **Fig. 7** Infiltration-profile scenario analysis based on the data collected during the first irrigation  
680 event performed at farm 1 in 2007. The real case is depicted in box (a) whilst the simulated cases,  
681 obtained by modifying the soil and irrigation parameters, are shown in boxes (b to h). The values of  
682 the parameters for the scenarios are listed in each single box: initial soil water content ( $\theta_i$ ), watering  
683 volume ( $V_d$ ), flow rate ( $F_r$ ) and irrigation duration ( $t_{ir}$ ).

684 (a) The circles represent the depths of water infiltration measured using the TDR technique. The  
685 dotted vertical line and dashed vertical line indicate the locations of the two TDR probe profiles,  
686 which were located at 30 m and 32 m from the beginning of the field, respectively.

## 687 TABLE CAPTIONS

688 **Tab. 1** Saturated and field-capacity water content values of the examined soils.

689 **Tab. 2** Soil texture and the percentages of stones in the three different farm soils monitored.

690 **Tab. 3** Plot size variability during the three-year monitoring period.

691 **Tab. 4** Relationship between the water volume stored on the surface ( $V_s$ ) and the water volume  
692 stored in the root layer ( $V_{rr}$ ) for the fifteen monitored irrigation events.

693 **Tab. 5** Calculated values of the dimensionless parameters  $t_k$  (-),  $C_k$  (-), and  $x_k$  (-) for the Philip and  
694 Farrell analytical solution.

695 **Tab. 6** Field-equivalent saturated hydraulic conductivity values ( $\text{cm h}^{-1}$ ) calculated for each farm  
696 and each year during the period from 2006-2008.

697 **Tab. 7** Saturated hydraulic conductivity values ( $\text{cm h}^{-1}$ ) estimated by means of the three BEST tests  
698 for each farm and each year during the period from 2006-2008. Differences between estimated  
699 saturated hydraulic conductivity and corresponding  $K_{Seq}$  values are given in brackets as percentage  
700 of saturated hydraulic conductivity.

701 **Tab. 8** RMSE calculated between the  $K_{Seq}$  values and the  $K_S$  values estimated by pedotransfer  
702 functions and BEST tests.

703 **Tab. 9** Differences between simulated and measured infiltration depths. The differences were  
704 calculated at 180 s ( $t_1$ ), 360 s ( $t_2$ ), 540 s ( $t_3$ ), 720 s ( $t_4$ ) from the start of the irrigation events and at  
705 the end of them ( $t_{ir}$ ) at the locations of the TDR profiles (30 m -  $x_1$  - and 32 m -  $x_2$  - from the  
706 beginning of the field).

707 **Tab. 10** Volumetric soil water content at the beginning of the irrigation event ( $\theta_i$ ), irrigation water  
708 volume ( $V_d$ ), flow rate ( $F_r$ ), irrigation event duration ( $t_{ir}$ ), time required for the water front to reach  
709 the end of the field ( $t_f$ ), field length ( $F_l$ ), and values of the water application efficiency ( $E_a$ ), water  
710 storage efficiency ( $E_s$ ), and water distribution efficiency ( $E_d$ ) for each irrigation event monitored  
711 during the period from 2006-2008.

712 **Tab. 11** Volumetric soil water content at the beginning of each irrigation event ( $\theta_i$ ), irrigation water  
713 volume ( $V_d$ ), flow rate ( $F_r$ ), irrigation event duration ( $t_{ir}$ ), field length ( $F_l$ ), and values of the water  
714 application efficiency ( $E_a$ ), water storage efficiency ( $E_s$ ), and water distribution efficiency ( $E_d$ ) for  
715 the first irrigation event performed at farm 1 in 2007 and the seven simulated scenarios.

716 **TABLES**

717

	Saturated soil water content (m <sup>3</sup> m <sup>-3</sup> )				Field capacity soil water content (m <sup>3</sup> m <sup>-3</sup> )			
	2006	2007	2008	Average	2006	2007	2008	Average
<b>Farm 1</b>	0.405	0.398	0.424	0.409	0.347	0.341	0.363	0.350
<b>Farm 2</b>	0.454	0.419	0.440	0.438	0.391	0.361	0.379	0.377
<b>Farm 3</b>	0.426	0.414	0.427	0.422	0.381	0.371	0.382	0.378

718 **Table 1**

719

Farm	Sand (%)	Silt (%)	Clay (%)	Stones (%)	Texture
<b>1</b>	20.4	71.1	8.5	20	Silty Loam
<b>2</b>	42.1	48.8	9.1	30	Loam
<b>3</b>	46.8	42.2	11	25	Loam

724 **Table 2**

725

Farm	2006		2007		2008	
	Length (m)	Width (m)	Length (m)	Width (m)	Length (m)	Width (m)
<b>1</b>	130	35	88	35	88	35
<b>2</b>	134	120	134	120	229	11
<b>3</b>	600	96	600	96	600	96

726 **Table 3**

727

	Irrigation event - year	$V_s/V_{rt}$ ( $m^3 m^{-3}$ )
<b>Farm 1</b>	1 - 2006	0.10
	4 - 2006	0.04
	1 - 2007	0.06
	2 - 2007	0.09
	1 - 2008	0.09
<b>Farm 2</b>	2 - 2006	0.10
	3 - 2006	0.10
	1 - 2007	0.10
	1 - 2008	0.03
<b>Farm 3</b>	2 - 2006	0.04
	4 - 2006	0.05
	1 - 2007	0.05
	2 - 2007	0.10
	1 - 2008	0.08
	4 - 2008	0.10

728 **Table 4**  
729

	<b>Farm 1</b>		<b>Farm 2</b>			<b>Farm 3</b>								
	<b>2006</b>		<b>2007</b>	<b>2008</b>		<b>2006</b>		<b>2007</b>	<b>2008</b>					
	<b>1</b>	<b>4</b>	<b>1</b>	<b>2</b>	<b>3</b>	<b>1</b>	<b>1</b>	<b>2</b>	<b>4</b>					
$\tau_k$	0.01	0.01	0.01	0.01	0.02	0.01	0.02	0.02	0.03	0.03	0.03	0.03	0.04	0.04
$C_k$	0.21	0.11	0.07	0.07	0.19	0.1	0.15	0.14	0.13	0.11	0.13	0.12	0.16	0.15
$x_k$	0.05	0.10	0.10	0.09	0.07	0.19	0.10	0.13	0.12	0.23	0.22	0.26	0.18	0.23

738 **Table 5**  
739

	<b>2006</b>	<b>2007</b>	<b>2008</b>	<b>Average</b>	<b>Standard deviation</b>
<b>Farm 1</b>	2.47	2.38	2.51	2.45	0.12
<b>Farm 2</b>	4.64	5.02	1.76	3.81	1.17
<b>Farm 3</b>	2.28	2.52	2.85	2.55	0.30

740 **Table 6**  
741



742

	BEST test 1			BEST test 2			BEST test 3		
	2006	2007	2008	2006	2007	2008	2006	2007	2008
<b>Farm 1</b>	2.34 (5.3%)	2.31 (2.9%)	2.25 (10.4%)	2.41 (2.4%)	2.44 (-2.5%)	2.48 (1.2%)	2.63 (-6.5%)	2.52 (-7.1%)	2.57 (-2.4%)
<b>Farm 2</b>	3.96 (14.7%)	3.18 (36.7%)	1.61 (8.5%)	4.35 (6.3%)	4.28 (14.7%)	1.87 (-6.3%)	4.66 (-0.4%)	4.91 (-40.9%)	2.48 (2.2%)
<b>Farm 3</b>	1.93 (15.7%)	2.36 (7.8%)	2.51 (12.2%)	2.16 (5.7%)	2.48 (3.1%)	2.73 (4.5%)	2.54 (-10.9%)	2.51 (2.0%)	3.07 (-7.3%)

743  
744

**Table 7**

	Ks_C	Ks_S	Ks_B	Ks_F	Ks_CS	Ks_P	Ks_DP	Ks_BEST #1	Ks_BEST #2	Ks_BEST #3
<b>RMSE</b>	1.54	2.73	3.06	2.49	3.00	0.62	6.10	0.69	0.28	0.28

745  
746

**Table 8**

		$t_1$	$t_2$	$t_3$	$t_4$	$t_{ir}$
<b>Farm 1</b> $x_1$	1 - 2006	0.012	0.009	0.005	-0.005	-0.012
	4 - 2006	0.006	0.007	0.006	0.003	-0.002
	1 - 2007	0.003	0.005	-0.009	-0.013	-0.013
	2 - 2007	0.006	-0.003	0.004	-0.004	-0.005
	1 - 2008	0.007	0.005	0.004	-0.007	-0.006
<b>Farm 1</b> $x_2$	1 - 2006	0.008	0.006	0.007	-0.003	-0.093
	4 - 2006	0.003	0.008	0.007	0.004	-0.007
	1 - 2007	0.006	0.002	0.002	-0.005	-0.004
	2 - 2007	0.007	0.004	0.005	-0.004	0.003
	1 - 2008	0.011	0.01	0.012	0.009	0.004
<b>Farm 2</b> $x_1$	2 - 2006	0.007	0.004	-0.005	0.006	0.01
	3 - 2006	0.006	0.006	0.007	-0.004	-0.018
	1 - 2007	0.011	0.018	0.004	-0.006	-0.004
	1 - 2008	0.01	0.007	0.005	-0.008	-0.005
<b>Farm 2</b> $x_2$	2 - 2006	0.006	-0.003	-0.008	-0.009	-0.012
	3 - 2006	0.004	0.004	0.002	-0.003	-0.007
	1 - 2007	0.018	0.011	0.006	-0.003	-0.008
	1 - 2008	0.007	0.013	0.01	0.005	0.005
<b>Farm 3</b> $x_1$	1 - 2006	0.003	0.003	0.005	-0.006	-0.008
	4 - 2006	0.009	0.008	0.01	-0.004	-0.005
	1 - 2007	0.004	0.007	0.011	0.008	-0.006
	2 - 2007	0.011	0.012	0.015	0.003	-0.01
	1 - 2008	-0.017	-0.018	-0.005	-0.003	0.012
	4 - 2008	-0.008	-0.007	-0.005	-0.011	0.007
<b>Farm 3</b> $x_2$	1 - 2006	0.011	0.009	0.006	0.004	-0.009
	4 - 2006	0.007	0.012	0.008	-0.005	-0.004
	1 - 2007	-0.006	0.004	0.012	0.009	-0.009
	2 - 2007	0.012	0.011	0.009	0.004	-0.006
	1 - 2008	-0.01	-0.01	-0.006	-0.003	0.011
	4 - 2008	-0.007	-0.006	-0.003	-0.008	0.009

747 **Table 9**  
748

	Monitored irrigation event - year	$\theta_i$ ( $\text{m}^3 \text{ m}^{-3}$ )	$V_d$ ( $\text{m}^3 \text{ ha}^{-1}$ )	$F_r$ ( $\text{m}^3 \text{ s}^{-1}$ )	$t_{ir}$ (s)	$t_{fl}$ (s)	$F_l$ (m)	$E_a$ (-)	$E_s$ (-)	$E_d$ (-)
Farm 1	1 - 2006	0.08	838	0.054	1513	1505	130	1.00	0.67	0.47
	4 - 2006	0.12	741	0.048	1505	1505	130	1.00	0.63	0.46
	1 - 2007	0.12	706	0.051	913	594	88	0.92	0.81	0.70
	2 - 2007	0.08	706	0.051	913	675	88	0.95	0.59	0.64
	1 - 2008	0.14	1482	0.060	1630	467	88	0.67	0.87	0.89
Farm 2	2 - 2006	0.05	1772	0.125	1797	1034	130	0.72	0.99	0.97
	3 - 2006	0.13	1183	0.125	1200	843	130	0.81	0.96	0.86
	1 - 2007	0.12	1119	0.125	1135	898	130	0.72	0.98	0.92
	1 - 2008	0.13	1817	0.160	2925	784	229	0.53	1.00	1.00
Farm 3	2 - 2006	0.12	1352	0.123	3957	3825	600	0.79	0.93	0.72
	4 - 2006	0.16	1409	0.128	3963	3144	600	0.69	0.98	0.93
	1 - 2007	0.08	1829	0.138	4771	3727	600	0.69	0.98	0.94
	2 - 2007	0.13	1577	0.159	3571	2326	600	0.65	1.00	0.99
	1 - 2008	0.07	2249	0.156	5190	3543	600	0.59	1.00	1.00
	4 - 2008	0.18	1791	0.161	4005	2250	600	0.60	1.00	1.00

749 **Table 10**

750

	Irrigation event - year	$\theta_i$ ( $\text{m}^3 \text{ m}^{-3}$ )	$V_d$ ( $\text{m}^3 \text{ ha}^{-1}$ )	$F_r$ ( $\text{m}^3 \text{ s}^{-1}$ )	$t$ (s)	$F_l$ (m)	$E_a$ (-)	$E_s$ (-)	$E_d$ (-)
Farm 1	2 - 2007 - real case	0.12	706	0.051	913	88	0.92	0.81	0.70
	2 - 2007 - case 1	0.12	727	0.040	1200	88	0.95	0.87	0.64
	2 - 2007 - case 2	0.12	970	0.040	1600	88	0.79	0.97	0.89
	2 - 2007 - case 3	0.12	1236	0.051	1600	88	0.64	1.00	0.89
	2 - 2007 - case 4	0.12	830	0.060	913	88	0.80	0.84	0.89
	2 - 2007 - case 5	0.12	968	0.070	913	88	0.71	0.86	0.89
	2 - 2007 - case 6	0.05	706	0.051	913	88	0.97	0.70	0.61
	2 - 2007 - case 7	0.15	706	0.051	913	88	0.86	0.92	0.79

760 **Table 11**

761

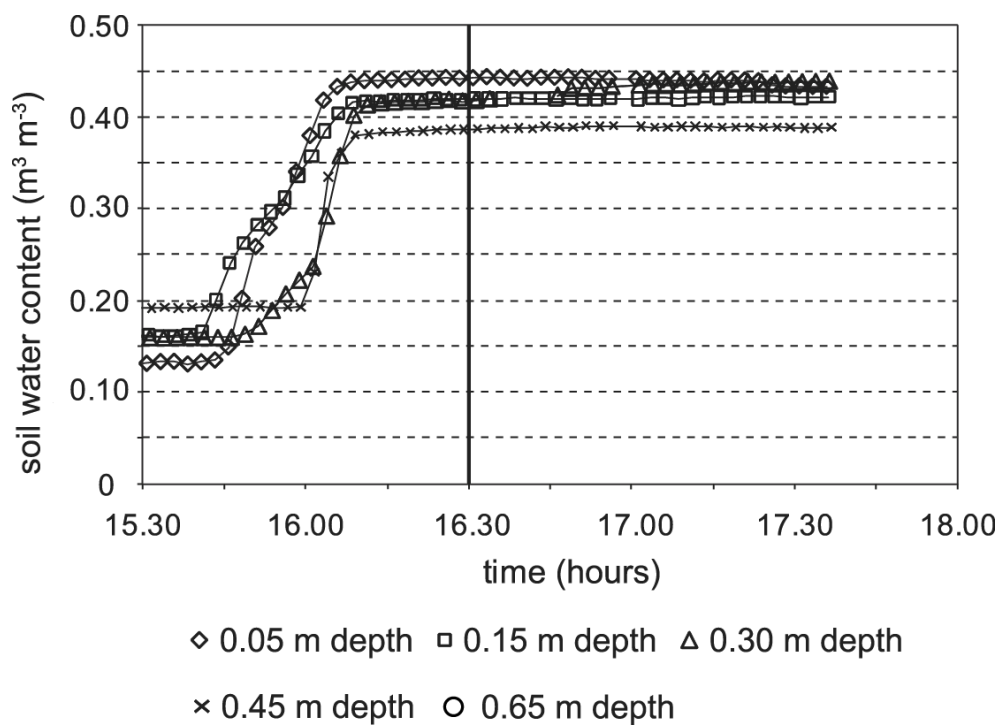


Figure 1

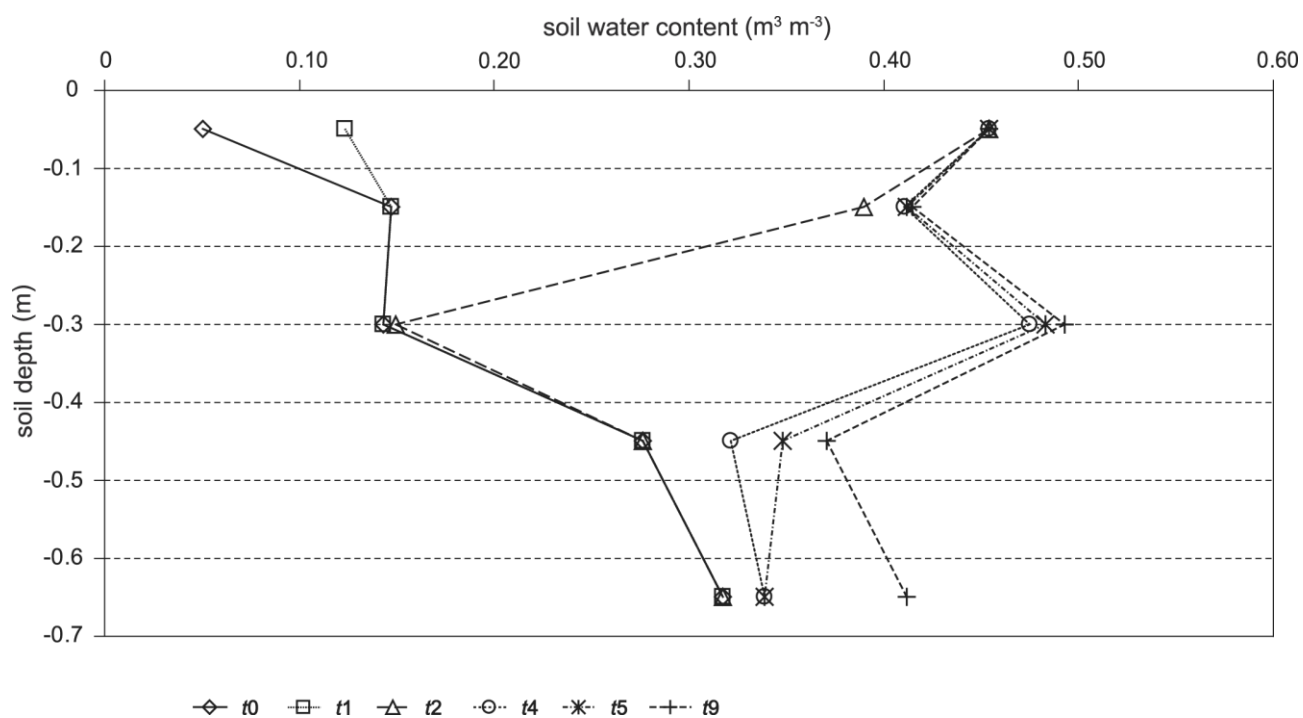
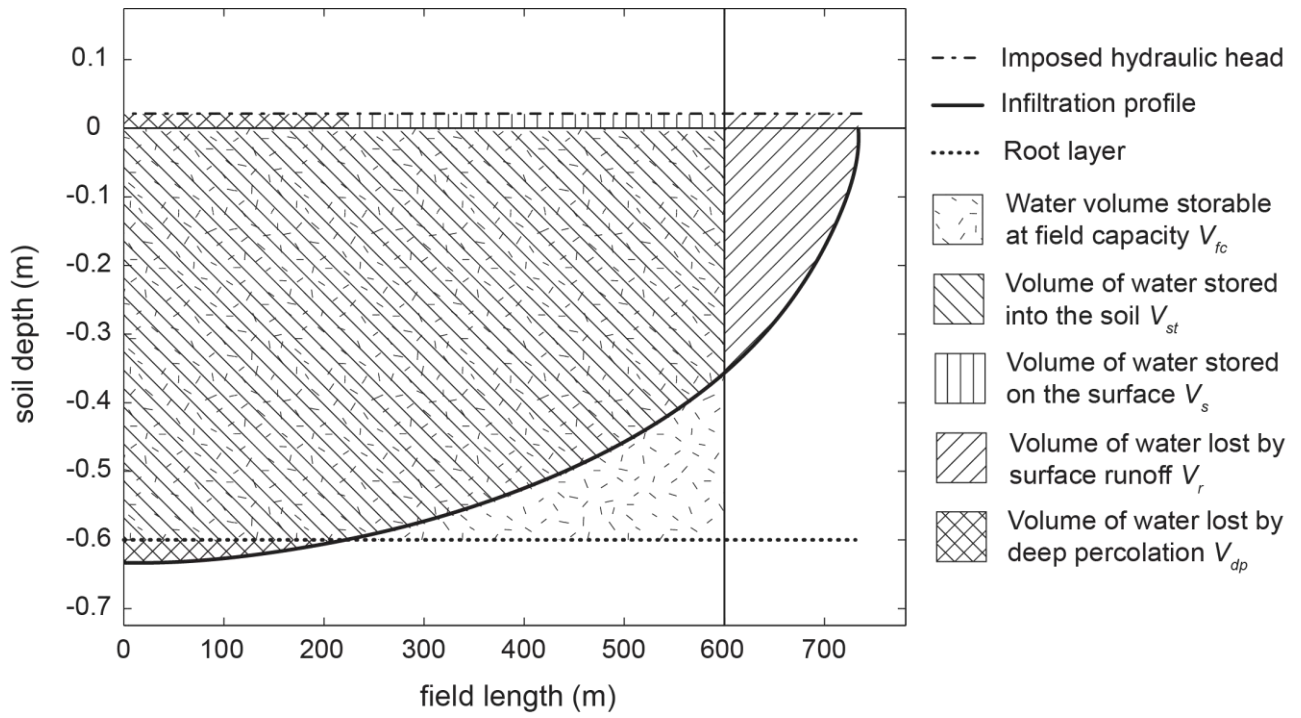
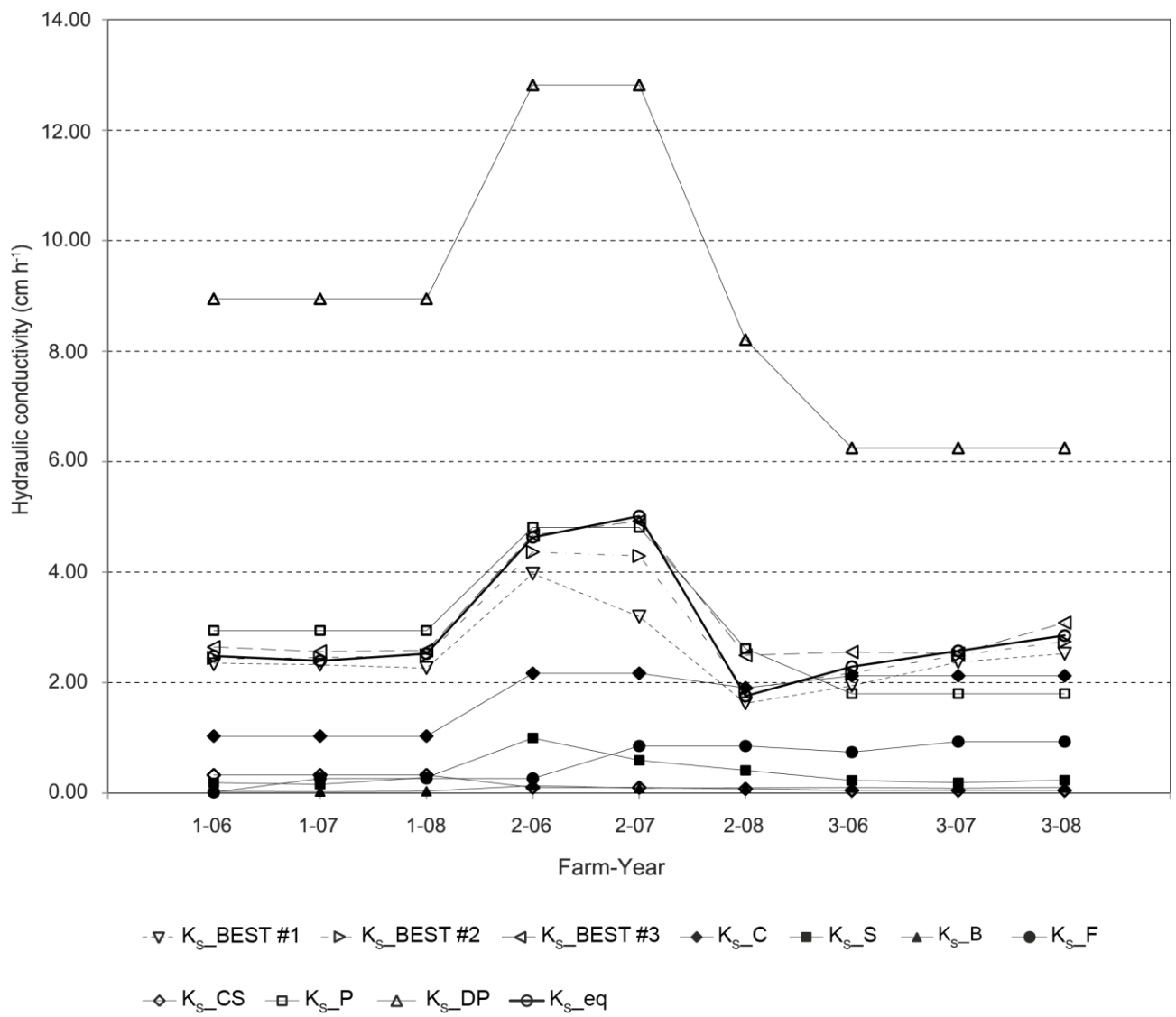


Figure 2



**Figure 3**



**Figure 4**

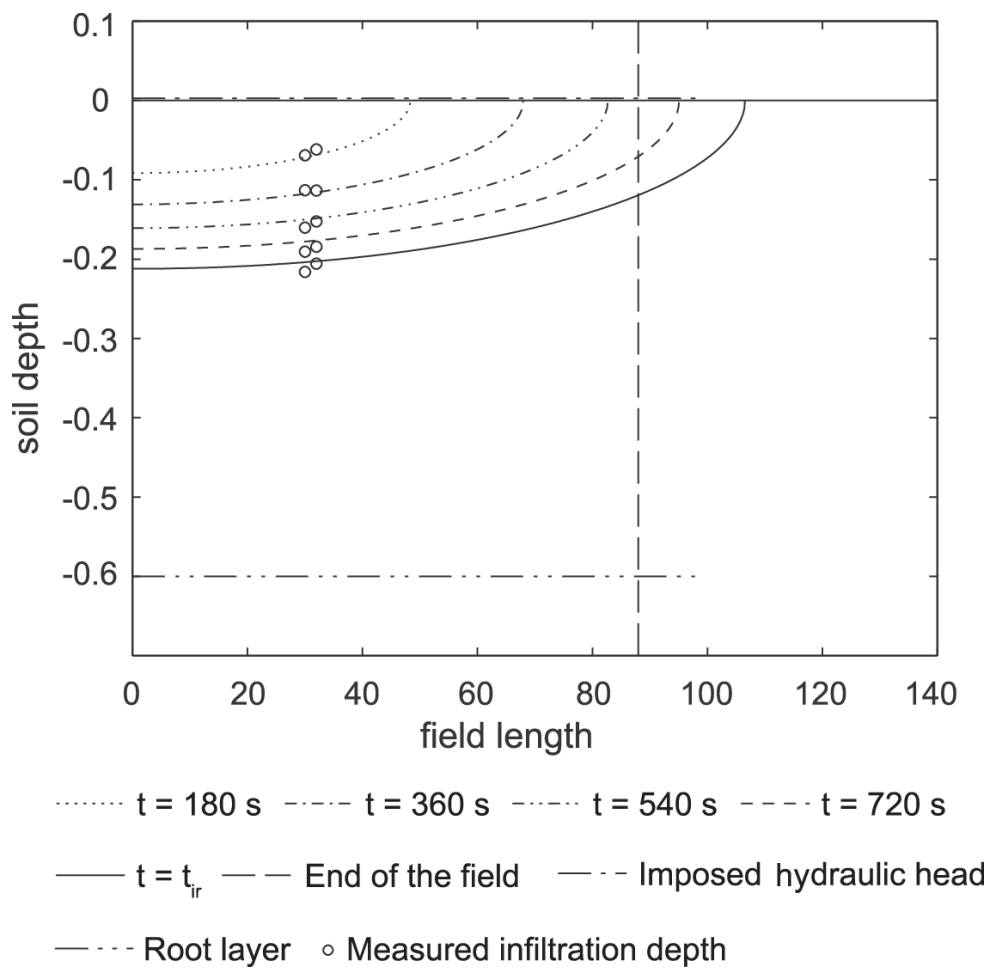


**Figure 5**

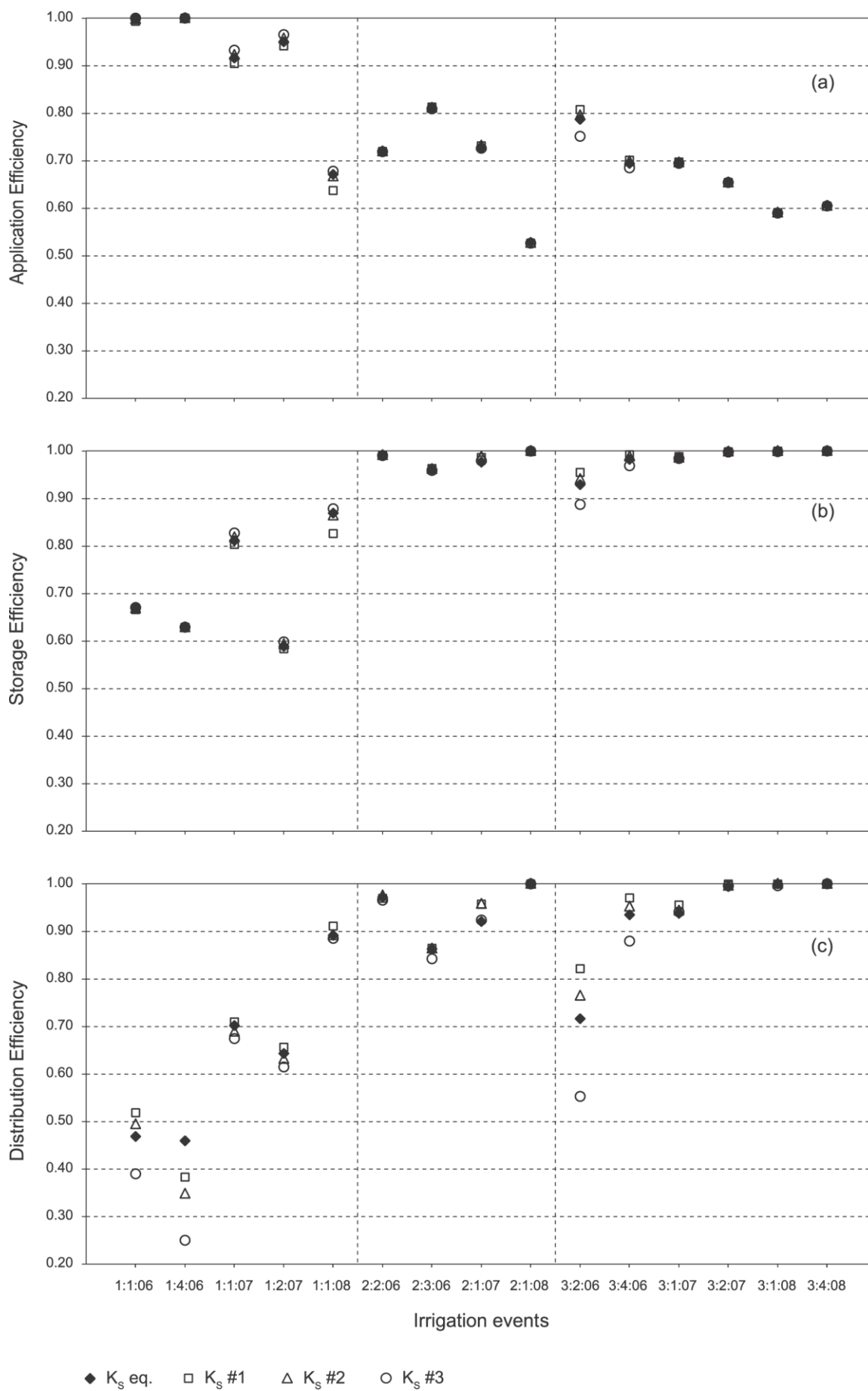


**Figure 6**



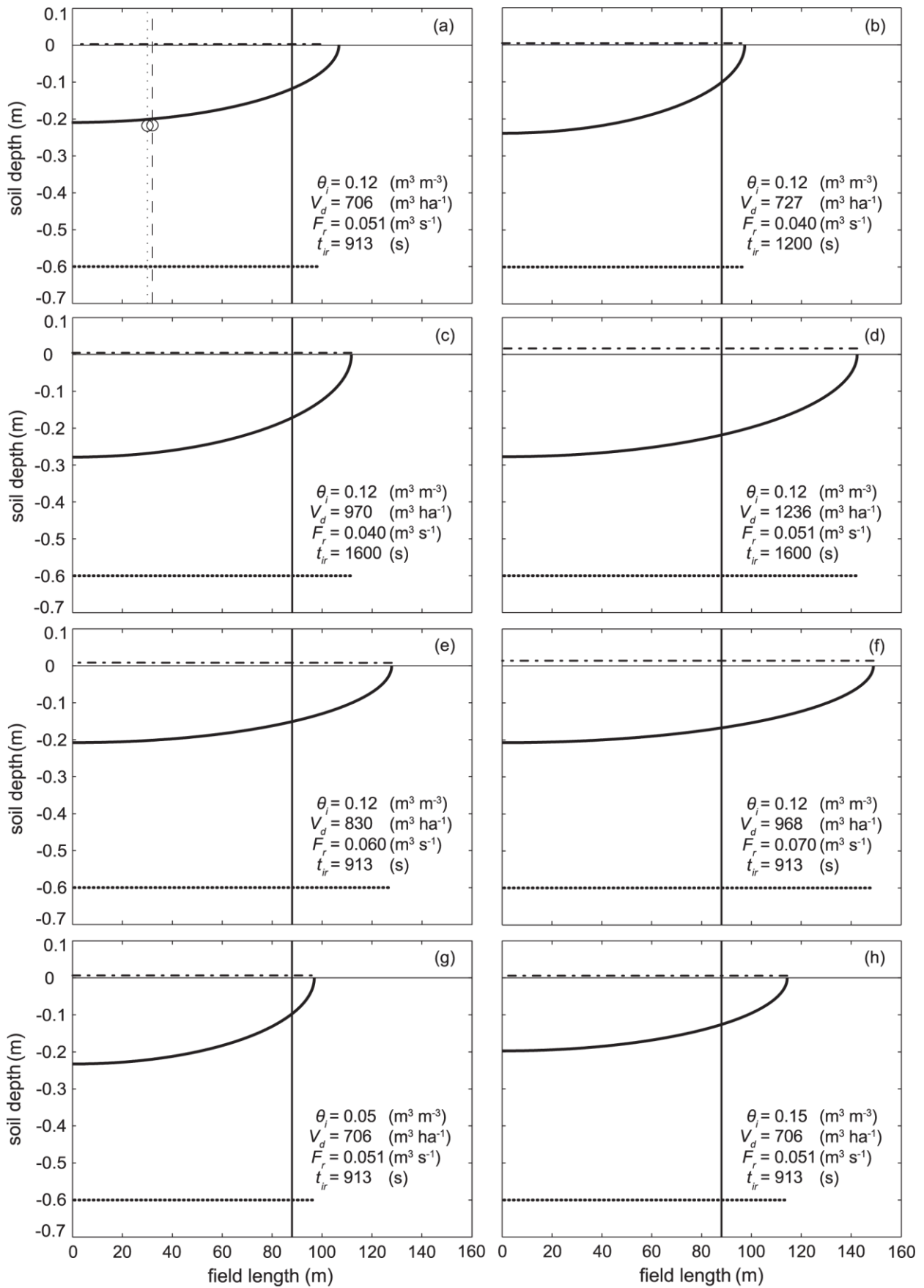


Figure 7